Hindawi Publishing Corporation
Mathematical Problems in Engineering
Volume 2016, Article ID 3734258, 13 pages
http://dx.doi.org/10.1155/2016/3734258

Research Article

Novel Damage Detection Techniques for Structural Health Monitoring Using a Hybrid Sensor

Dengjiang Wang, Jingjing He, Banglin Dong, Xiaopeng Liu, and Weifang Zhang

School of Reliability and Systems Engineering, Beihang University, 37 Xueyuan Road, Haidian District, Beijing 100191, China

Correspondence should be addressed to Jingjing He; hejingjing@buaa.edu.cn

Received 19 February 2016; Revised 30 March 2016; Accepted 4 April 2016

Academic Editor: Wenyu Zhao

This study presents a technique for detecting fatigue cracks based on a hybrid sensor monitoring system consisting of a combination of intelligent coating monitoring (ICM) and piezoelectric transducer (PZT) sensors. An experimental procedure using this hybrid sensor system was designed to monitor the cracks generated by fatigue testing in plate structures. A probability of detection (POD) model that quantifies the reliability of damage detection for a specific sensor or the nondestructive testing (NDT) method was used to evaluate the weight factor for the ICM and PZT sensors. To estimate the uncertainty of model parameters in this study, the Bayesian method was employed. Realistic data from fatigue testing was used to validate the overall method, and the results show that the novel damage detection technique using a hybrid sensor can quantify fatigue cracks more accurately than results obtained by conventional sensor methods.

1. Introduction

Fatigue damage for complex structures has become a crucial subject in the study of structural safety, and it is an important influencing factor on the costs of life-cycle management in civil, aviation, marine, and power generation structures [1–3]. Structural health monitoring (SHM) is an effective method of diagnosing fatigue damage. In order to detect fatigue damage, the following NDT methods have been applied in SHM: ultrasonic inspection, magnetic particle inspection, electromagnetic inspection, radiographic inspection, and visual inspection [4–6]. Devices for traditional NDT methods are usually complex and expensive. In recent years, several new monitoring methods have been proposed, including Lamb-wave-based PZT sensors [7], fibre Bragg gratings (FBGs) [8], and intelligent coating monitoring (ICM) [9, 10].

In SHM systems, a single sensor or one indicator is usually applied to diagnose the damage in structures. Different sensors offer different features in damage detection. For example, the use of Lamb waves with PZT sensors has drawn extensive attention from the SHM community. Many studies have dealt with the practical applications of PZT wafers in specific target systems, for example, plates and beam structures [11, 12]. FBGs are immune to electromagnetic interference (EMI) and loop influences. They are lightweight and have small physical dimensions, which suits their need to be embedded into, or attached to, a structure [8]. Strain and temperature have so far been the dominating measurements of interest for FBG [13]. Acoustic emission techniques (AET) have a great potential in structural health monitoring. For example, AET can detect cracks and wire breaks [14].

However, different sensor techniques applied in SHM systems suffer from their physical limitations, such as operation requirement and measurement range [15–17]. The use of hybrid sensors is a new technique that combines different sensors. This technique overcomes the limitations of every single sensor technique and can provide accurate and reliable structural health monitoring results. A hybrid sensor system was developed to detect the elastic waves launched by a PZT actuator using a high-speed and high-accuracy FBG sensor [18]. The hybrid sensor system with simplified devices can detect the debonding and delamination at the interfaces of the laminate in bonded structures with high accuracy. A hybrid PZT/fibre optic scheme was proposed that used a PZT to generate a controlled excitation to a structure and fibre optic sensors to capture the response of the corresponding

structure [19]. Hybrid sensor systems have been applied to aerospace vehicles and structures for quick nondestructive evaluation and long-term health monitoring. The reliability of the monitoring system is enhanced as the hybrid sensor system combines the information obtained from different sensors. Furthermore, comparison of time series obtained by recording different physical quantities resulted in a drastic improvement of reliability and lowered the detection threshold of deterioration [14].

ICM is a type of intelligent material that adheres to the surface of a structure [20]. It can directly indicate the damage in a structure based on the attached feature of coating and has no effect on the integrity of the structure. One of the major advantages for ICM is that it can detect damage in locations with poor accessibility (e.g., inside the fuel tank of an aircraft). Numerous applications in difficult-to-access locations on commercial and military aircraft have validated the effectiveness and reliability of ICM for structural health monitoring [21]. Nevertheless, there are also some limitations for ICM-based damage detection; it can only be applied on the condition that the damage location has been evaluated beforehand. Moreover, it can only offer an approximation of crack size due to its sensor configuration. The problems of missing detection and false alarms also widely restrict its application [21].

Unlike ICM, a Lamb-wave-based PZT sensor can locate and quantify structural damage. Studies show that Lamb-wave-based PZT sensor detection has great potential in SHM systems [22–24]. The propagation of Lamb waves in a structure results in the mode conversion of wave energy into different modes, and the changes in Lamb wave signals can be used to interrogate structural integrity [25, 26]. In particular, it is very suitable to detect material discontinuity on components with a simple geometry, such as a plate with a centre hole. With a designed PZT sensor layout, the location and severity of the damage can be estimated by specific algorithms. Many advanced signal-processing techniques have been used to process Lamb wave data, such as wavelet and Hilbert transforms [27, 28]. The remaining challenge for the Lamb-wave-based PZT sensor is how to accurately locate and quantify damage [29, 30]. In this study, a novel hybrid sensor system using both ICM and PZT is proposed to detect cracks for structural health monitoring. A crack quantification model using signal features and POD results from both ICM and PZT sensors is proposed to perform damage detection. The Bayesian method was employed to evaluate uncertainties for the hybrid sensor damage detection method.

The paper is organized as follows. First, a brief introduction about the ICM and PZT sensors is presented, and the POD method for each sensor is established. Then the Bayesian method is proposed to estimate the POD model parameters. Then, a crack quantification model using damage-sensitive features from both ICM and PZT sensors is developed to perform damage detection. Finally, a hybrid sensor monitoring experiment is included and the experimental data are applied to verify the effectiveness of the hybrid sensor monitoring strategy.

2. Methodology Development

In this study, a novel hybrid sensor system using both ICM and PZT is proposed to detect cracks for structural health monitoring. The POD concept is used to quantify the reliability of damage detection using ICM and PZT methods separately. After that, the weight factor is proposed to represent the reliability of detection based on POD results from both sensor techniques. A crack quantification model using signal features from both ICM and PZT sensors is proposed to perform damage detection based on the weight factor. Ideally, a large amount of experimental data is desired for an accurate and reliable POD model. However, the field structural health monitoring data in real-time is sparse for most of the engineering cases. In order to establish a reliable and comprehensive crack quantification model in view of sparse data, the Bayesian method is employed to estimate POD model parameters. An experimental procedure of the hybrid sensor is designed to validate the overall method. The overall flowchart of the proposed damage detection technique using a hybrid sensor is shown in Figure 1.

2.1. Intelligent Coating Sensor. The intelligent coating monitoring (ICM) sensor is a new functional gradient material characterized by a thin-film material, which when applied to a structure can directly detect any existing damage in the structure by sensing layers of resistance in the coating [10]. The intelligent coating sensor consists of three layers: a driving layer, a sensing layer, and a protective layer [20, 21]. The driving layer is made up of insulating materials that play two roles: (1) a crack will appear on the driving layer when the substrate is damaged, and the crack will split the sensing layer at the same time, and (2) the highly insulated driving layer can separate the substrate and the sensing layer. The sensing layer is made up of a conductive material. As cracks appear in the substrate, the resistance value of the sensing layer increases. The protective layer is used to protect the internal sensing layer. The structure of intelligent coating sensor is shown in Figure 2.

A crack is indicated when the resistance of the coated area is larger than a predefined threshold value. ICM-based damage detection can only be applied when the damage location has been previously identified. For most ICM-related damage detection research, changes in the features of the coating material are used to reveal the existence of damage [9]; very little research has been performed on crack size quantification using ICM.

2.2. Lamb Wave Data for the PZT Sensor. Lamb-wave-based PZT sensors have shown great potential in nondestructive evaluations and structural health monitoring systems. Lamb waves allow for the evaluation of large areas in a short time period for both isotropic and anisotropic materials [31]. The mechanism for Lamb wave damage quantification is to identify discontinuities in the wave propagation paths that alter the characteristics of transmitted/deflected waves [32]. Compared with the A_0 mode, the fundamental symmetrical mode (S_0) of Lamb waves can detect the through-thickness

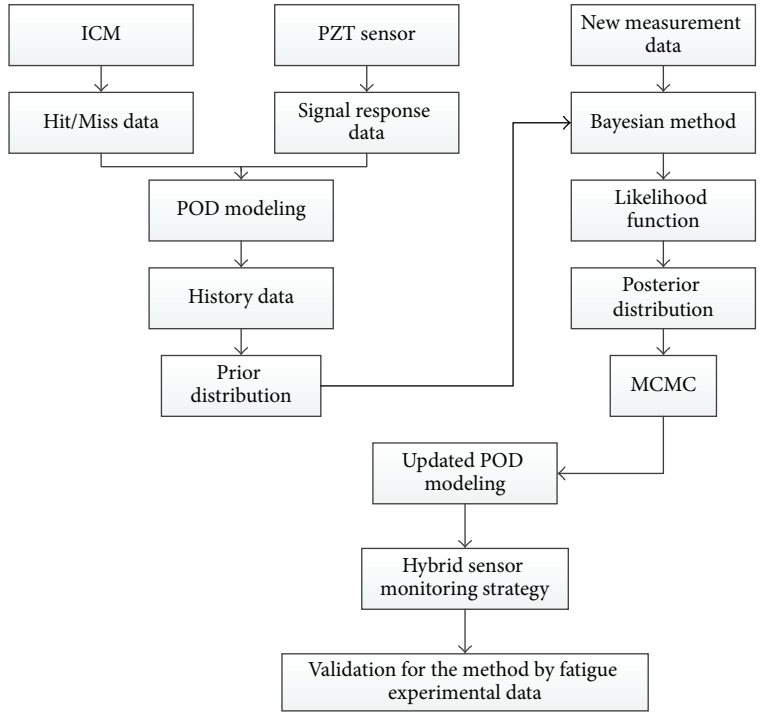

FIGURE 1: The overall diagram of the POD model-based hybrid sensor monitoring method.

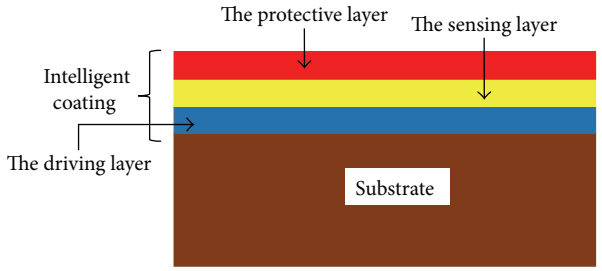

FIGURE 2: The structure of the ICM sensor.

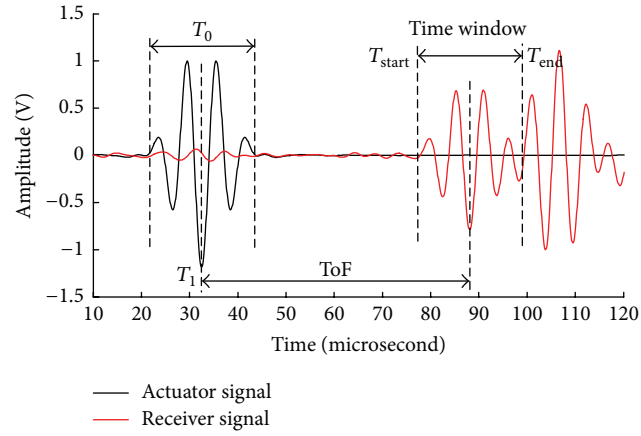

FIGURE 3: Schematic illustration for the time window calculation.

cracks more accurately [24, 33–35]. The first wave package of the S_0 mode is chosen to extract damage-sensitive features from the data. The group velocity is verified in an undamaged specimen by measuring the time of flight (ToF) between two sensors with a known distance. The signal envelope is calculated using the Hilbert transform. The calculated time window is the time duration between T_{start} and T_{end}; the two terms are given, respectively, as follows:

$$T_{start} = T_1 + \text{ToF} - \frac{1}{2}T_0, \quad (1)$$

$$T_{end} = T_1 + \text{ToF} + \frac{1}{2}T_0, \quad (2)$$

where T_1 represents wave excitation time of an actuator, ToF is the time of flight from an actuator to a receiver, and T_0 is the period of excitation wave envelope. The time window is illustrated in Figure 3.

As mentioned in [36], a single feature is not sufficient to develop the crack quantification model using specimens with the same geometry and configuration due to the inter-specimen variability. In this study, two features of Lamb wave data are proposed to quantify the damage; namely, signal normalized amplitude and signal phase change based on the following hypothesis. The wave amplitude reflects the energy retained after transmission over a discontinuity. A large discontinuity is expected to disperse more amplitude of the wave. The phase change due to a change of traveling path and distance of the wave is affected by different discontinuities, that is, different crack sizes. Based on the two

damage-sensitive features, the crack quantification model can be illustrated as

$$\hat{a} = \varphi_0 + \varphi_1 N + \varphi_2 P + \varphi_3 N \cdot P, \tag{3}$$

where $\hat{a}$ represents the predicted crack size, N represents the normalized amplitude, P represents the phase change, and φ_i, $i = 0, 1, 2, 3$, are fitting parameters.

The ICM sensor technique indicates the existence of cracks in structures based directly on a structure's effect on the attached coating. On the other hand, a PZT sensor evaluates a crack size based on changes of Lamb wave signals. In order to combine the two sensors, a weight factor is proposed to represent the reliability of detection based on the POD results from both sensor techniques. A crack quantification model using signal features from both is proposed to perform damage detection based on the weight factor.

2.3. POD Modelling. The POD is a rational way to assess the performance of the detection reliability of a given inspection technique. There are two methods to produce POD curves, which are functions of flaw size [37, 38]. First, NDT results were only recorded to indicate whether the flaw was detected or not. This type of data is called Hit/Miss data. This way of recording data is appropriate for some NDT methods (e.g., penetrant testing or magnetic particle testing); however, there is more information in the NDT response in many NDT systems (e.g., peak voltage in eddy current NDT and the signal amplitude in ultrasonic NDT). Since the NDT signal response can be interpreted as a perceived flaw size or defect severity, the data is called signal response data. For the ICM method, the measured data belong to the Hit/Miss data, while the measured data of the PZT sensor belong to signal response data. This study establishes POD models for ICM and PZT sensors.

2.3.1. Hit/Miss Data for ICM. The ICM method only records the resistance of layer sensing, assuming that when a recorded resistance value is larger than a predefined threshold, a crack is detected. However, the accuracy of measurements is questionable due to the uncertainties associated with sensor manufacturing, specimen properties, and human factor. The POD model of ICM was established to quantify the reliability of the ICM method when used to detect the specified size of a crack.

The experimental data of ICM only records whether a crack has or has not been reported. Thus, the POD modelling for Hit/Miss data was adopted for ICM. For Hit/Miss data, the log-odd model [39], lognormal model [40], and exponential model [41, 42] are commonly used. Considering this factor, the modified log-odd POD model is expressed as

$$\mathrm{POD}(a) = \frac{\exp\left(\gamma_1 + \gamma_2 \ln\left(a - a_{\mathrm{th}}\right)\right)}{1 + \exp\left(\gamma_1 + \gamma_2 \ln\left(a - a_{\mathrm{th}}\right)\right)}, \tag{4}$$

where γ_1 and γ_2 are the fitting parameters, a is the actual crack size, and a_{th} is the minimum crack size detected (for the ICM sensors used in this study, the width was 0.5 mm). The ICM sensor gave an alarm when a crack propagated through the sensor. Therefore, the theoretic minimum crack size detected by the intelligent coating sensor was set to 0.5 mm.

2.3.2. Signal Response Data for the PZT Sensor. Generally, there are two configurations for PZT sensors, namely, pulse-echo configuration and pitch-catch configuration [36]. The pitch-catch configuration was chosen in this study. In the pitch-catch configuration, the actuator and the receiver are placed across the potential damage region. When a crack exists in the potential damage region, the discontinuities in the wave propagation paths will alter the characteristics of the transmitted/deflected waves. Two signal features of Lamb waves are extracted in this study (normalized amplitude and phase change). Based on the changes of the two signal features, a data-driven crack quantification model was established; therefore, the measurement data of Lamb wave analysis are regarded as signal response data.

The POD model for signal response data can be derived from the correlation of the predicted crack size $\hat{a}$ and the actual crack size a. It has been reported that $\ln a$ and $\ln \hat{a}$ are usually log linearly correlated through the following equation [43, 44]:

$$\ln \hat{a} = \alpha + \beta \ln a + \varepsilon, \tag{5}$$

where α and β are fitting parameters and ε is a normal random variable with zero mean and standard deviation σ_ε. A predefined term $\hat{a}_{\mathrm{th}}$ is used to represent the detection threshold, which is usually determined by the measured noises and physical limits of the measuring devices.

This detection threshold affects the minimum detectable size and the probability of false positive detection [45, 46]. The crack is considered to be detected when the reported value $\hat{a}$ is larger than the threshold value $\hat{a}_{\mathrm{th}}$. The probability of detection can then be expressed as

$$\begin{aligned} \mathrm{POD}(a) &= \Pr\left(\alpha + \beta \ln a + \varepsilon > \ln \hat{a}_{\mathrm{th}}\right) \\ &= \Phi\left(\frac{\ln a - \left(\ln \hat{a}_{\mathrm{th}} - \alpha\right)/\beta}{\sigma_\varepsilon/\beta}\right), \end{aligned} \tag{6}$$

where $\Pr(\cdot)$ represents the probability of event $(\cdot)$ and $\Phi(\cdot)$ represents the standard normal cumulative distribution function.

Ideally, a large amount of experimental data is desired for an accurate and reliable POD model. However, the field structural health monitoring data in real-time was sparse for most of the engineering cases. In order to establish a reliable and comprehensive crack quantification model in view of the sparse data, the Bayesian method was employed to estimate the POD model parameters.

2.4. Bayesian Method. Conventional crack quantification methods are based on existing knowledge about the experimental data, while the sparse existing knowledge is not sufficient to fit the parameters of the model. The uncertainties of many factors may cause errors in existing knowledge. For many engineering problems, usage monitoring or inspection data are usually available at a regular time interval in

either SHM systems or nondestructive inspections. As new information is gathered, it can be used to update the initial estimation of the quantification model and POD model. The critical issue is how to combine historical data with new data. The Bayesian method is a method of statistical inference in which Bayes' theorem is used to update the probability for a hypothesis.

Consider a quantification model $F(\mathbf{X};\mathbf{Y})$ to quantify the variable d, where $\mathbf{X}$ is an uncertain parameter vector that needs to be updated by the Bayesian method and $\mathbf{Y}$ is an independent variable vector. In an ideal condition, one obtains $d = F(\mathbf{X};\mathbf{Y})$. Due to the natural uncertainties, an error e needs to be included to describe the quantification model.

Using the Bayesian method to incorporate the error e, a prior distribution $p(\mathbf{X} \mid F)$ and likelihood function $p(d \mid \mathbf{X}, F)$ are used to deduce the posterior distribution

$$p(\mathbf{X} \mid d, F) = \frac{p(\mathbf{X} \mid F)\, p(d \mid \mathbf{X}, F)}{p(d \mid F)}. \tag{7}$$

The model error has intrinsic uncertainty: modelling uncertainty and measurement uncertainty for the probabilistic modelling. For the purpose of illustration, the model error e is assumed to be a zero-mean normal variable with standard deviations of σ_e [47]:

$$p(d \mid \mathbf{X}) = \frac{1}{\sqrt{2\pi\sigma_e^2}} \exp\left\{\frac{-\left[d - F(X;Y)^2\right]}{2\sigma_e^2}\right\}. \tag{8}$$

2.4.1. Noninformation Prior. If no information is known about the value of a parameter, then a noninformative prior is used. The expression for noninformation prior is

$$p(\mathbf{X}, \sigma_e \mid d, F) \propto \frac{1}{\sigma_e} \prod_{i=1}^{n} \frac{1}{\sqrt{2\pi\sigma_e^2}} \exp\left\{\frac{-\left[d_i - F_i(\mathbf{X};Y)^2\right]}{2\sigma_e^2}\right\}, \tag{9}$$

where d_i and F_i are the i_{th} real testing data and predicted data and n is the total number of measurements.

2.4.2. Informative Prior. The prior distribution gives numerical information that is crucial to the estimation of the model. This would be a traditional informative prior, which might come from a literature review or explicitly from an earlier data analysis. With prior information and measured data, the posterior distribution of $(\mathbf{X}, \sigma_e)$ reads

$$p(\mathbf{X}, \sigma_e \mid d, F) \propto p_0(\mathbf{X}, \sigma_e \mid d, F) \cdot \prod_{i=1}^{n} \frac{1}{\sqrt{2\pi\sigma_e^2}} \exp\left\{\frac{-\left[d_i - F_i(X;Y)^2\right]}{2\sigma_e^2}\right\}. \tag{10}$$

For the prior information $p_0(\mathbf{X}, \sigma_e \mid d, F)$, a maximum likelihood estimator can be used to fit, and $\mathbf{X}$ is an independent multivariate normal distribution:

$$p_0(\mathbf{X}, \sigma_e \mid d, F) = \frac{1}{2\pi\sqrt{|\Sigma_0|}} \cdot \exp\left\{-\frac{1}{2}\left[(\mathbf{X}, \sigma_e) - \mu_0\right]\Sigma_0^{-1}\left[(\mathbf{X}, \sigma_e) - \mu_0\right]^T\right\}, \tag{11}$$

where μ_0 is a mean vector and Σ_0 is a covariance matrix for the estimated vector.

2.5. Hybrid Sensor Monitoring Method. With a predefined threshold, ICM can indicate a crack with a specified size that exists in the substrate. Based on signal response data, the PZT sensor can predict the crack size by measuring signal features. The POD concept is used to quantify the reliability of damage detection using the ICM and PZT methods separately. In order to incorporate the ICM and PZT sensors data, a weight factor is proposed to represent the reliability of detection based on POD results from both sensor techniques. A crack quantification model using signal features from the ICM and PZT sensors is proposed to perform damage detection based on the weight factor

$$a = \xi_1 a_1 + \xi_2 a_2, \tag{12}$$

where a_1 is the crack size reported by the ICM, a_2 is the crack size predicted by the PZT sensor, and ξ_1 and ξ_2 are weight factors calculated by POD models:

$$\xi_1 = \frac{\text{POD (ICM)}}{\text{POD (ICM)} + \text{POD (PZT sensor)}}, \qquad \xi_2 = \frac{\text{POD(PZT sensor)}}{\text{POD (ICM)} + \text{POD (PZT sensor)}}. \tag{13}$$

3. Hybrid Sensor Damage Detection Experiment

In order to validate the effectiveness of the proposed damage detection method by a hybrid sensor, an experiment with naturally generated fatigue crack was designed. Both ICM and PZT sensors were used to monitor the crack propagation produced by cyclic fatigue loading.

3.1. Specimen. In this study, the material of specimen was Al 7050-T6, and its density, elasticity modulus, and Poisson ratio were 2.83 g/cm^3, 71.7 GPa, and 0.33, respectively. The geometry of the specimen was 600 × 300 × 2 mm with a 10 mm through-hole in the centre. Parallel to the shorter side of the specimen, on each side of the hole, a 3 mm notch was introduced using electrical discharge machining (EDM). Figure 4 provides a schematic of the specimen.

3.2. Sensor Layout. Both the ICM and PZT sensors were used on the specimen to build the hybrid sensor network for damage detection using combined damage-sensitive features.

Table 1: Actual crack sizes when 16 ICM sensor alarms are activated.

Number	1	2	3	4	5	6	7	8
Crack size (mm)	5.332	5.523	5.713	6.501	7.144	9.104	10.137	11.400
Number	9	10	11	12	13	14	15	16
Crack size (mm)	14.15	16.106	17.017	17.541	19.024	20.322	21.425	22.174

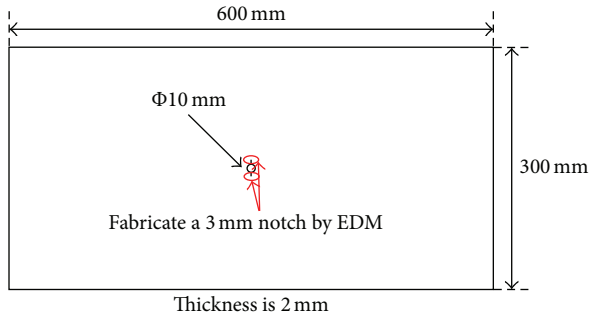

Figure 4: Specimen schematic.

The ICM sensor was applied on front side of the specimen, while the back side was monitored by the PZT sensor.

ICM only reveals the existence of a crack. Its accuracy is dependent on many factors, such as the thickness of the specimen and the preset threshold of resistance value. In order to detect different crack sizes, 16 ICM sensors were uniformly installed with a centre-to-centre distance of 1.4 mm. The first ICM sensor was placed next to the EDM notch, and the layout of the ICM sensor is shown in Figure 5(a).

The PZT sensor network design is critical for Lamb-wave-based damage detection. In general, the strategy of sensor network for the Lamb wave method can be classified into two categories: pulse-echo configuration and pitch-catch configuration [7]. For pulse-echo configuration, the actuators and the receivers need to be placed on one side of the test area. This configuration is not suitable for remote detection of damage due to the superposition by reflection signals of boundary. The actuators and the receivers were therefore placed on both sides of the test area in the pitch-catch configuration. Since less-reflected signals of boundaries are superimposed, the pitch-catch configuration provides more sensitivity to detect cracks in remote areas. Therefore, the pitch-catch configuration was used in this study, and the layout of the PZT sensors is shown in Figure 5(b).

3.3. Experiment Process. The overall experimental setup of the hybrid sensor consists of three parts: the hybrid sensor monitoring system, the hydraulic fatigue testing system, and the data acquisition and process system. The experimental flowchart is shown in Figure 6.

The hybrid sensor monitoring system contains the ICM system and PZT sensor monitoring system. The hydraulic fatigue testing system includes the MTS testing machine, the MTS control system, a hydraulic clamping device, and a microscope. The microscope was used to measure the crack surface length, and, in this study, the average value of crack size measured by microscope was regarded as the actual crack size. The data acquisition and process system was applied to acquire the measurements, which include Lamb wave data of the PZT sensors and the resistance values of ICM. At the same time, crack sizes and their corresponding fatigue cycles were recorded as well. Figure 7 shows the experimental test equipment used.

A hydraulic fatigue machine was used to generate cyclic loads. Before crack initiation, the maximum stress was set to 90 MPa. When a crack appeared, the maximum stress was reduced to 75 MPa. The cycling frequency was 5 Hz, and the stress ratio was 0.1.

Existing literature has shown that when the product of frequency and plate thickness is 0.32 MHz mm, the group velocity of the S_0 mode for Lamb wave is almost a constant with slight dispersion [48]. Since the thickness of the specimen was 2 mm, the centre frequency was set to 0.16 MHz in this study. A Hamming-windowed sinusoidal tone burst with 3.5 cycles was used as the excitation signal. Baseline signals (without the presence of damage) and signals with damage were obtained using this configuration. The group velocity of S_0 mode used in this study was calculated as 5,252 m/s [31].

4. Crack Size Quantification Using the Hybrid Sensor Method

4.1. POD Modelling for ICM. In this study, 16 ICM sensors were installed at each side of an EDM notch as illustrated in Figure 5(a). When an ICM sensor alarm was activated, it indicated that a crack had propagated through the sensor. In order to report cracks with different sizes, ICM sensors were uniformly installed 1.4 mm between the centres of sensors. The ICM sensors and the actual crack size for 16 sensors are shown in Table 1. When the ICM sensor alarm was activated, the crack increment was equal to the real detected crack size minus the distance between the EDM notch and sensor's location. The crack increments of each ICM sensor were calculated using the same procedure in order to formulate the POD model. The ICM sensor could only indicate whether a crack did or did not exist in the substrate. Theoretically, an ICM alarm can report the occurrence of a constant crack increment due to the ICM sensor layout design of this study.

For ICM, no historical data is available for POD modelling. In order to establish a POD model for ICM, as mentioned above, the nonprior Bayesian method was used. Data of ten sensors were used to estimate the POD model for ICM by the Bayesian method, as expressed in (14). As illustrated in Figure 8, when the crack size was larger than 8 mm, almost all of the cracks can be detected by ICM.

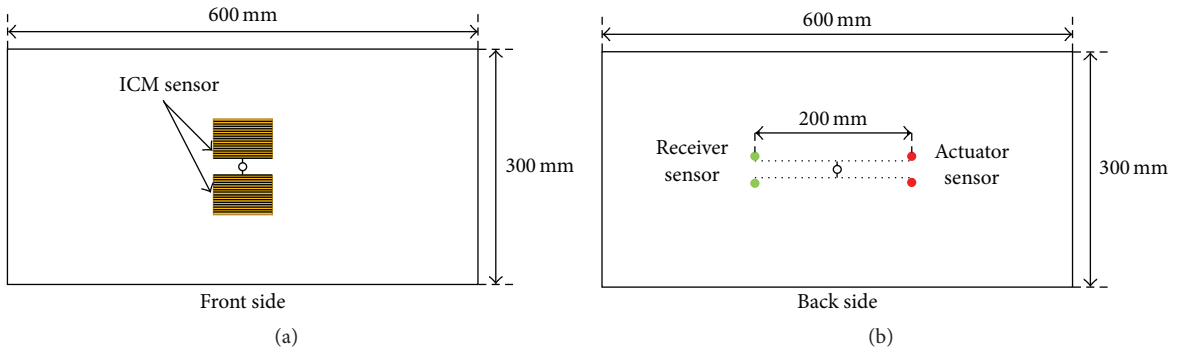

Figure 5: Sensors layout on specimen. (a) ICM in front side. (b) PZT sensors in back side.

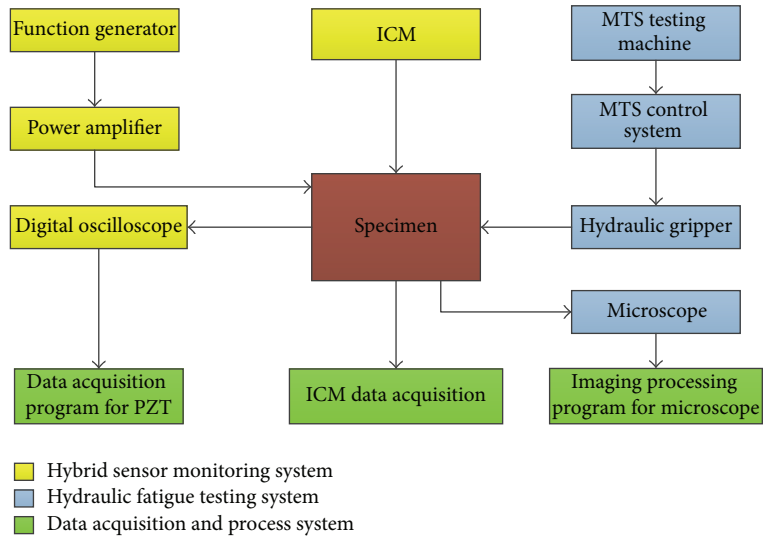

Figure 6: The experimental flowchart.

However, the POD is only 0.4 when the crack size is 2 mm. It can be seen from the results that the missing detection is a main problem in ICM system. Consider

$$\mathrm{POD}(a) = \frac{\exp(-1.7953 + 2.9205\ln(a - 0.5))}{1 + \exp(-1.7953 + 2.9205\ln(a - 0.5))}. \quad (14)$$

In order to formulate an accurate and reliable POD model, a large amount of experimental data is desired; however, in actual engineering cases, the experimental data for ICM is sparse. When new measurements are included, the POD model for ICM can be updated by the Bayesian method.

4.2. POD Modelling for a PZT Sensor

4.2.1. Information from a Previous Study. In order to establish a reliable and comprehensive POD model, experimental data from a previous study was employed as prior information. The data from hybrid sensor damage detection experiments was used as additional information to reduce the uncertainties from different sensor techniques due to the Bayesian method.

In a previous study, the in situ Lamb wave data from fatigue testing on an actual lap-joint component were obtained [36]. PZT sensors were employed to perform NDT during fatigue cyclical loading. The two signal features of Lamb wave (normalized amplitude and phase change) were extracted in order to quantify the crack. The crack initiation and propagation were monitored by optical microscope with a Charge Coupled Device (CCD) camera during the fatigue testing process. The details of the fatigue test can be found in [36]; the data of five specimens were used as prior information to establish the crack size quantification model and POD model.

The signal features of Lamb wave (normalized amplitude and phase change) in [36] were used to establish a crack quantification model, and this model was regarded as prior information. The least-square-fit method was used to estimate the fitting parameters in crack quantification model (see (3)):

$$\hat{a} = 7.9846 - 7.2906N - 2.143P + 7.8598N \cdot P, \quad (15)$$

where N, P, and $\hat{a}$ have the same physical definitions as in (3).

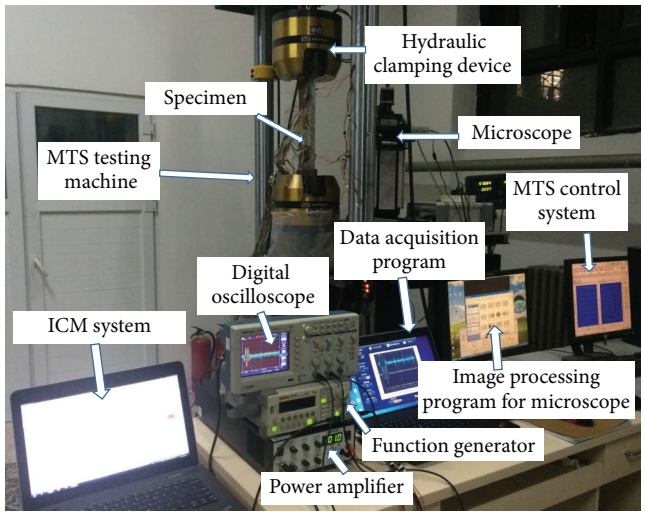

FIGURE 7: Test equipment for the hybrid sensor damage detection system.

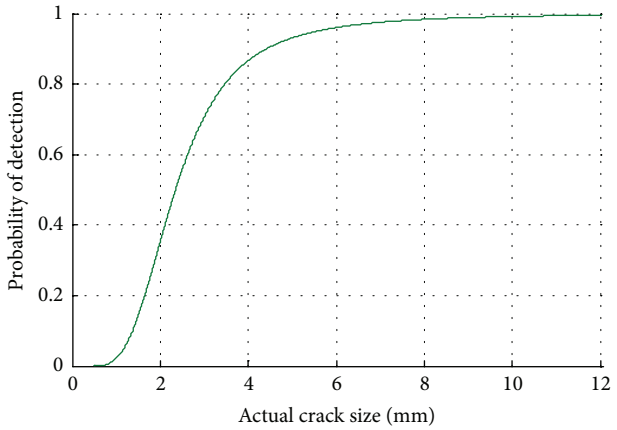

FIGURE 8: The results of POD models for ICM with nonprior information.

4.2.2. POD Model Parameter Updating Using the Bayesian Method. All 13 Lamb wave measurements were obtained from the hybrid sensor damage detection experiment described in Section 3 (illustrated in Figure 9 with the scattering in the data by error bars).

For each point illustrated in Figure 9, the S_0 wave package of the Lamb wave had been extracted according to (1)-(2), as shown in Figure 10.

The same signal features (normalized amplitude and phase change) of Lamb waves recorded in the plate fatigue experiment were also used here, as shown in Figure 11.

The crack quantification model (see (15)) based on the previous study was used to predict the experimental data of the Lamb waves obtained in this study. The actual crack size and the predicted crack size based on (15) are illustrated in Figure 12(a). The results demonstrated in Figure 12(a) show that the crack quantification model obtained from previous study could not be directly applied to new measurement data. The poor performance of the crack quantification model

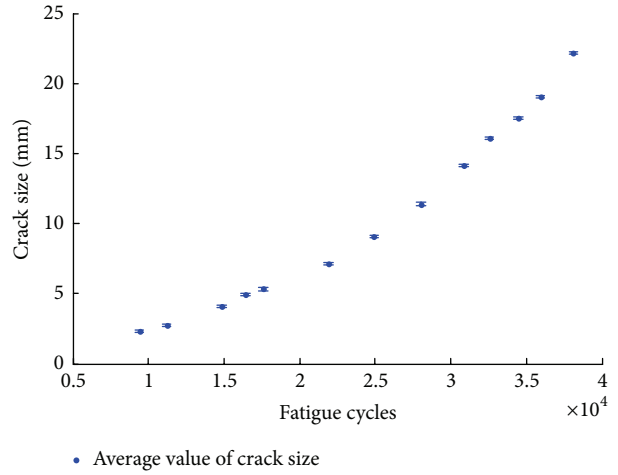

FIGURE 9: Crack size measured by microscope and fatigue cycles.

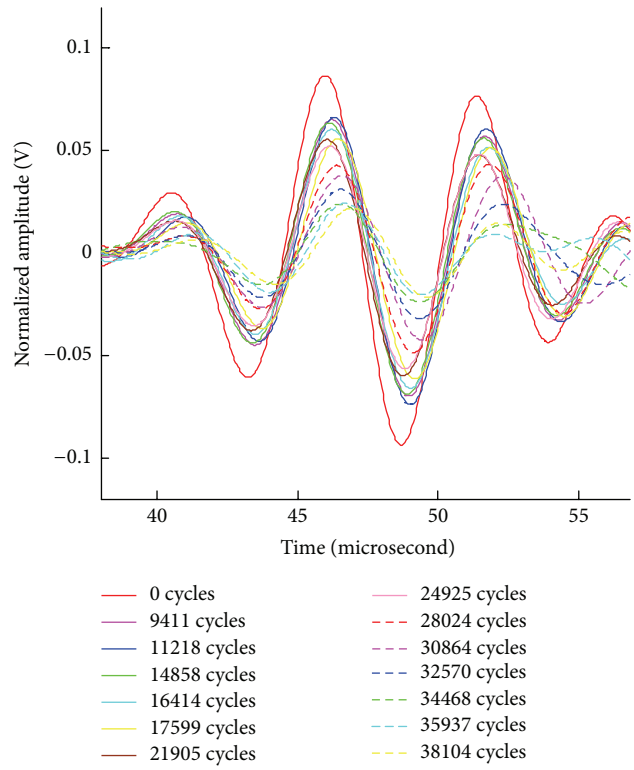

FIGURE 10: The S_0 package of the Lamb wave at each measured point.

would yield an inaccurate POD model. In order to establish a reliable and comprehensive POD model, the Bayesian method was employed to reduce the uncertainties caused by factors such as different specimen geometry, different fatigue testing environment, and human factors. First, five new measurements were used to update the crack quantification model and results are shown in Figure 12(b). Figure 12(c) demonstrates the prediction results when parameters were updated by ten measurements. As a result, as shown in Figure 12(c), the performance of the crack quantification model was significantly improved.

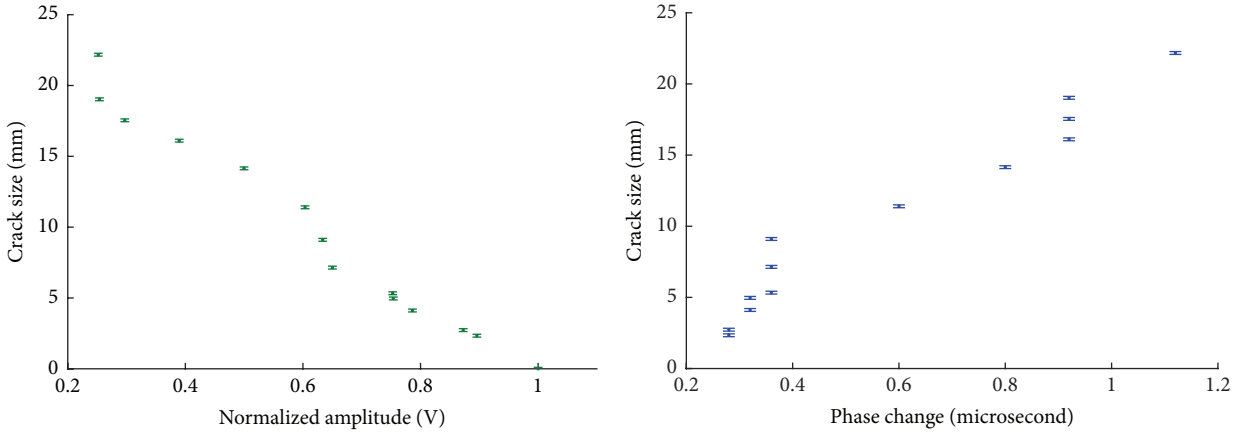

Figure 11: The crack size and damage-sensitive features of Lamb waves: (a) normalized amplitude and (b) phase change.

Updated by ten measurements, the parameters for (15) are expressed as

$$\hat{a} = 9.4528 - 12.7810N + 8.6646P + 10.6268N \cdot P, \quad (16)$$

where N, P, and $\hat{a}$ have the same physical definitions as in (3).

The predicted crack size can be calculated by (16). Based on the predicted crack size and actual crack size, the POD model can be expressed as

$$\mathrm{POD}(a) = \Phi\left(\frac{\ln a - 0.4094}{0.14}\right). \quad (17)$$

Figure 13 is the POD curve after updating with ten measurements.

According to Figure 13, the probability of detection is close to 1 when the crack size is larger than 2 mm. Comparing the POD results for ICM (Figure 8) with that of the PZT sensor (Figure 13), the Lamb-wave-based damage detection method performed better in identifying small cracks.

4.3. Crack Quantification Using the Hybrid Sensors Strategy. In this section, a crack quantification model using signal features and POD results from both ICM and PZT sensors is proposed. The results of the two POD models in (14) and (17) were used as weight factors, which can be evaluated by (13). The crack quantification model using the proposed hybrid sensor strategy is

$$\begin{aligned} a = {} & \frac{\exp\left(-1.7953 + 2.9205\ln\left(a_1 - 0.5\right)\right)/\left(1 + \exp\left(-1.7953 + 2.9205\ln\left(a_1 - 0.5\right)\right)\right),}{\exp\left(-1.7953 + 2.9205\ln\left(a_1 - 0.5\right)\right)/\left(1 + \exp\left(-1.7953 + 2.9205\ln\left(a_1 - 0.5\right)\right)\right) + \Phi\left(\left(\ln a_2 - 0.4094\right)/0.14\right)} a_1 \\ & + \frac{\Phi\left(\left(\ln a_2 - 0.4094\right)/0.14\right)}{\exp\left(-1.7953 + 2.9205\ln\left(a_1 - 0.5\right)\right)/\left(1 + \exp\left(1.7953 + 2.9205\ln\left(a_1 - 0.5\right)\right)\right) + \Phi\left(\left(\ln a_2 - 0.4094\right)/0.14\right)} a_2, \end{aligned} \quad (18)$$

where a_1 and a_2 have the same physical definitions as in (12).

As illustrated in Figure 14, the last three data points, which are monitored by ICM and PZT sensors simultaneously, are used to validate the overall proposed method. The relative error applies to evaluate the accuracy of the crack quantification model, and the relative error φ is defined in (19) as

$$\varphi = \left|\frac{\hat{a} - a}{a}\right| \times 100\%, \quad (19)$$

where $\hat{a}$ is the predicted crack size and a is the actual crack size.

The predicted results for single sensors and hybrid sensors are illustrated in Table 2. Results show that the novel damage detection technique using a hybrid sensor can predict the crack size more accurately as the relative errors are all below 6%.

The novel damage detection method combines the data measured by ICM and PZT sensors based on the POD results. There are two aspects that may affect the prediction performance of the proposed method: (1) the damage-sensitive features which are identified by each single sensor and the physical models which are chosen to correlate the damage-sensitive features and crack size and (2) the reliability of damage detection methods for each type of sensors measured by POD results. The key idea of the proposed method is to perform crack size prediction using damage-sensitive features and POD results from both ICM and PZT sensors. The proposed method is not limited to a specific crack size

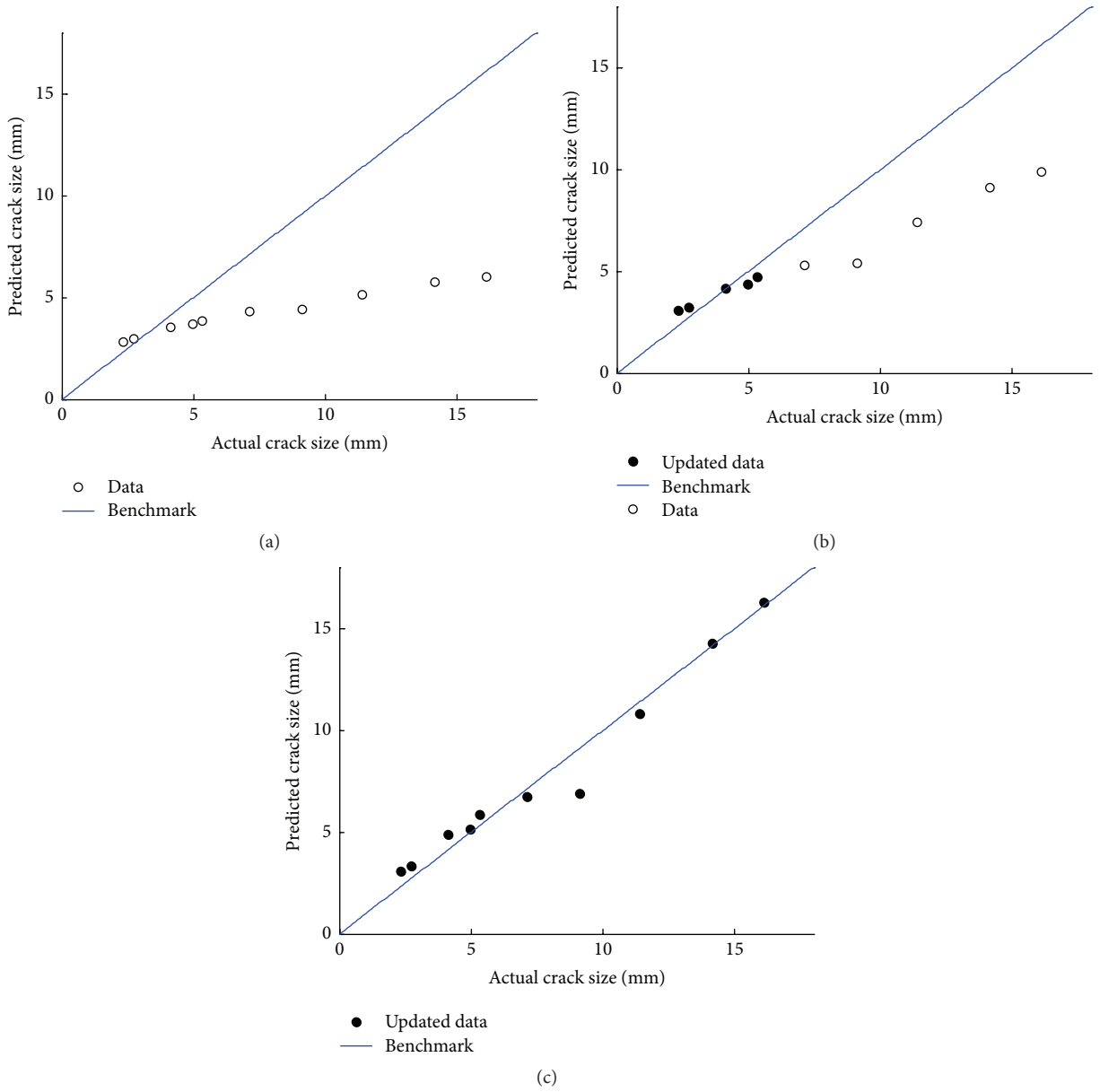

Figure 12: Bayesian updated results with experiment data of hybrid sensor. (a) No data was used for updating, (b) updating with five measurements, and (c) updating with ten measurements.

Table 2: Predicted results for single sensors and hybrid sensors.

Data	Actual crack size	ICM		PZT		Hybrid sensor	
		Reported crack size	Relative error	Predicted crack size	Relative error	Predicted crack size	Relative error
I	17.541 mm	19.15 mm	9.17%	16.532 mm	5.75%	17.405 mm	0.78%
II	19.024 mm	20.55 mm	8.02%	16.661 mm	12.42%	17.958 mm	5.6%
III	22.174 mm	24.75 mm	11.62%	18.936 mm	14.6%	20.875 mm	5.86%

quantification model for each sensor. Any damage-sensitive feature and the physical model which are suitable for a target system can be used. Therefore, the underestimation of predicted results in Table 2 is not caused by the proposed method. Take Data I in Table 2 as an example; when the phase change of Lamb-wave-based PZT sensor increased by 0.1 microseconds, the crack size predicted by PZT sensor is 16.768 mm. Based on calculations, the crack size predicted by hybrid sensor is 17.563 mm, which is larger than the actual crack size (17.541 mm).

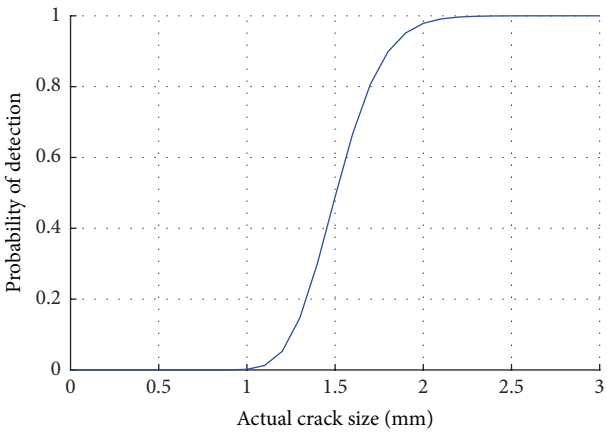

Figure 13: POD model after updating with ten measurements.

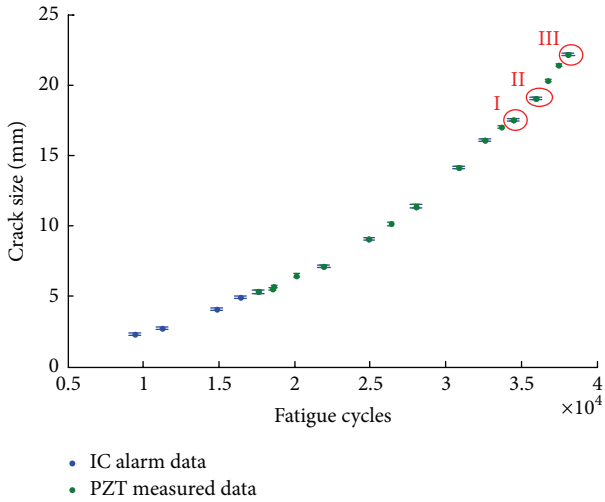

Figure 14: Data used to validate the proposed method.

5. Conclusion

This study presents a novel damage detection technique using a hybrid sensor that combines ICM and PZT sensors. POD models were established to evaluate the detection reliability of each sensor. A crack quantification model using damage-sensitive features and POD results from both ICM and PZT sensors was proposed. The Bayesian method was used to estimate and update the required but uncertain model parameters. The ICM and PZT sensors were used simultaneously to monitor the cracks produced by natural fatigue testing and the overall method was validated by natural fatigue testing data. Results demonstrated that the hybrid sensor method can quantify fatigue crack more accurately than those methods where only one type of sensors was used.

Competing Interests

The authors declare that they have no competing interests.

Acknowledgments

The research work of this study was supported by fund from the National Natural Science Foundation of China (Grant no. 11404018). The support is gratefully acknowledged.

References

[1] G. Sposito, C. Ward, P. Cawley, P. B. Nagy, and C. Scruby, "A review of non-destructive techniques for the detection of creep damage in power plant steels," *NDT & E International*, vol. 43, no. 7, pp. 555–567, 2010.

[2] R. S. Geng, "Modern acoustic emission technique and its application in aviation industry," *Ultrasonics*, vol. 44, pp. e1025–e1029, 2006.

[3] B. W. Drinkwater and P. D. Wilcox, "Ultrasonic arrays for non-destructive evaluation: a review," *NDT & E International*, vol. 39, no. 7, pp. 525–541, 2006.

[4] C. Segebade, "Nondestructive materials testing—overview and evaluation," in *Proceedings of the Annual Meeting on Nondestructive Materials Testing*, vol. 63, p. 617, 1997.

[5] M. P. Papaelias, C. Roberts, and C. L. Davis, "A review on non-destructive evaluation of rails: state-of-the-art and future development," *Proceedings of the Institution of Mechanical Engineers, Part F*, vol. 222, no. 4, pp. 367–384, 2008.

[6] H. E. Boyer and T. L. Gall, *Metals Handbook*, Desk Edition, 2nd edition, 1985.

[7] L. Y. Yu and V. Giurgiutiu, "In-situ optimized PWAS phased arrays for lamb wave structural health monitoring," *Journal of Mechanics of Materials and Structures*, vol. 2, no. 3, pp. 459–487, 2007.

[8] M. Majumder, T. K. Gangopadhyay, A. K. Chakraborty, K. Dasgupta, and D. K. Bhattacharya, "Fibre Bragg gratings in structural health monitoring-present status and applications," *Sensors and Actuators A: Physical*, vol. 147, no. 1, pp. 150–164, 2008.

[9] S. Z. Zhang, Y. J. Yan, and Z. Y. Wu, "Electric potential detection for structural surface crack using coating sensors," *Sensors and Actuators, A: Physical*, vol. 137, no. 2, pp. 223–229, 2007.

[10] Y. Sun and M. B. Liu, "Analysis of the crack penetration/deflection at the interfaces in the intelligent coating system utilizing virtual crack closure technique," *Engineering Fracture Mechanics*, vol. 133, pp. 152–162, 2015.

[11] Y. Feng, L. Zhou, and Z. Li, "Damage detection for plate-like structure using matching pursuits with chirplet atom," in *Sensors and Smart Structures Technologies for Civil, Mechanical, and Aerospace Systems*, vol. 7981 of *Proceedings of SPIE*, pp. 1–12, 2011.

[12] D. A. Saravanos and P. R. Heyliger, "Coupled layerwise analysis of composite beams with embedded piezoelectric sensors and actuators," *Journal of Intelligent Material Systems and Structures*, vol. 6, no. 3, pp. 350–363, 1995.

[13] H.-N. Li, D.-S. Li, and G.-B. Song, "Recent applications of fiber optic sensors to health monitoring in civil engineering," *Engineering Structures*, vol. 26, no. 11, pp. 1647–1657, 2004.

[14] C. Grosse, G. Mclaskey, S. Bachmaier, S. D. Glaser, M. Krüger, and C. Grosse, "A hybrid wireless sensor network for acoustic emission testing in SHM," in *Proceedings of the SPIE Sensors and Smart Structures Technologies for Civil, Mechanical, and Aerospace Systems*, 2008.

[15] M. P. Blodgett and P. B. Nagy, "Eddy current assessment of near-surface residual stress in shot-peened nickel-base superalloys," *Journal of Nondestructive Evaluation*, vol. 23, no. 3, pp. 107–123, 2004.

[16] A. Habibalahi, M. S. Safizadeh, A. Habibalahi, and M. S. Safizadeh, "Pulsed eddy current and ultrasonic data fusion applied to stress measurement," *Measurement Science & Technology*, vol. 25, pp. 1009–1016, 2014.

[17] M. L. Lobanov, I. P. Sysolyatina, V. K. Chistyakov et al., "On possibility of nondestructive testing of the grain size in the intermediate stages of manufacturing electrical steel," *Russian Journal of Nondestructive Testing*, vol. 39, no. 8, pp. 615–628, 2003.

[18] T. Ogisu, M. Shimanuki, S. Kiyoshima, Y. Okabe, and N. Takeda, "Development of damage monitoring system for aircraft structure using a PZT actuator/FBG sensor hybrid system," in *Smart Structures and Materials 2004: Industrial and Commercial Applications of Smart Structures Technologies*, vol. 5388 of *Proceedings of SPIE*, pp. 425–436, July 2004.

[19] X. Qing, A. Kumar, C. Zhang, I. F. Gonzalez, G. Guo, and F.-K. Chang, "A hybrid piezoelectric/fiber optic diagnostic system for structural health monitoring," *Smart Materials and Structures*, vol. 14, no. 3, pp. S98–S103, 2005.

[20] Z. Lü and M. Liu, "China Patent," No. 200610104559.4.

[21] F. Hu, M. Liu, G. Hong, and Z. Lü, "Flaw-detected coating sensors applied in aircraft R&M," in *Proceedings of the Annual Reliability and Maintainability Symposium (RAMS '09)*, pp. 95–99, Fort Worth, Tex, USA, January 2009.

[22] S. S. Kessler, S. M. Spearing, and C. Soutis, "Damage detection in composite materials using Lamb wave methods," *Smart Materials & Structures*, vol. 11, no. 2, pp. 269–278, 2002.

[23] Z. Su, L. Ye, and Y. Lu, "Guided Lamb waves for identification of damage in composite structures: a review," *Journal of Sound and Vibration*, vol. 295, no. 3–5, pp. 753–780, 2006.

[24] J.-B. Ihn and F.-K. Chang, "Pitch-catch active sensing methods in structural health monitoring for aircraft structures," *Structural Health Monitoring*, vol. 7, no. 1, pp. 5–19, 2008.

[25] Y. Feng, J. Yang, and W. Chen, "Delamination detection in composite beams using a transient wave analysis method," *Journal of Vibroengineering*, vol. 15, no. 1, pp. 139–151, 2013.

[26] L. Zhou, Z. He, and H. Sun, "Lamb wave mode conversion-based crack detection for plate-like structures without baseline information," *Journal of Vibroengineering*, vol. 15, no. 2, pp. 647–657, 2013.

[27] S. Grondel, C. Delebarre, J. Assaad, J.-P. Dupuis, and L. Reithler, "Fatigue crack monitoring of riveted aluminium strap joints by Lamb wave analysis and acoustic emission measurement techniques," *NDT & E International*, vol. 35, no. 3, pp. 137–146, 2002.

[28] K. S. Ho, D. R. Billson, and D. A. Hutchins, "Ultrasonic Lamb wave tomography using scanned EMATs and wavelet processing," *Nondestructive Testing and Evaluation*, vol. 22, no. 1, pp. 19–34, 2007.

[29] X. Chen, Y. Gao, and L. Bao, "Lamb wave signal retrieval by wavelet ridge," *Journal of Vibroengineering*, vol. 16, no. 1, pp. 464–476, 2014.

[30] A. Vilpišauskas and R. Kažys, "Investigation of air-coupled generation of asymmetric Lamb waves using rectangular phased arrays," *Journal of Vibroengineering*, vol. 16, no. 3, pp. 1397–1404, 2014.

[31] V. Giurgiutiu, "Tuned Lamb wave excitation and detection with piezoelectric wafer active sensors for structural health monitoring," *Journal of Intelligent Material Systems and Structures*, vol. 16, no. 4, pp. 291–305, 2005.

[32] Z. Chang and A. Mal, "Scattering of Lamb waves from a rivet hole with edge cracks," *Mechanics of Materials*, vol. 31, no. 3, pp. 197–204, 1999.

[33] S. S. Kessler, S. M. Spearing, and C. Soutis, "Structural health monitoring in composite materials using Lamb wave methods," in *Proceedings of the 16th Technical Conference of the American Society for Composites*, September 2001.

[34] D. N. Alleyne and P. Cawley, "The interaction of Lamb waves with defects," *IEEE Transactions on Ultrasonics, Ferroelectrics, and Frequency Control*, vol. 39, pp. 381–397, 1992.

[35] C. Wang and F. Chang, "Built-in diagnostics for impact damage identification of composite structures," in *Proceedings of the 2nd International Workshop on Structural Health Monitoring*, pp. 8–10, Stanford, Calif, USA, September 1999.

[36] J. He, X. Guan, T. Peng et al., "A multi-feature integration method for fatigue crack detection and crack length estimation in riveted lap joints using Lamb waves," *Smart Materials and Structures*, vol. 22, no. 10, Article ID 105007, 2013.

[37] K. Simola and U. Pulkkinen, "Models for non-destructive inspection data," *Reliability Engineering & System Safety*, vol. 60, no. 1, pp. 1–12, 1998.

[38] M. J. S. Lowe, R. E. Challis, and C. W. Chan, "The transmission of Lamb waves across adhesively bonded lap joints," *The Journal of the Acoustical Society of America*, vol. 107, no. 3, pp. 1333–1345, 2000.

[39] G. A. Georgiou, *Probability of Detection (PoD) Curves*, Jacobi Consulting, London, UK, 2006.

[40] C. Harding and G. Hugo, "Statistical analysis of probability of detection hit/miss data for small data sets," *AIP Conference Proceedings*, vol. 657, pp. 1838–1845, 2003.

[41] C.-H. Tsai and W.-F. Wu, "Application of probabilistic fracture mechanics to the risk assessment of pressure vessels," in *Transactions of the 12 International Conference on Structural Mechanics in Reactor Technology*, vol. 1000, pp. 135–140, 1993.

[42] R. Zheng and B. R. Ellingwood, "Role of non-destructive evaluation in time-dependent reliability analysis," *Structural Safety*, vol. 20, no. 4, pp. 325–339, 1998.

[43] A. P. Berens, "NDE reliability data analysis," in *ASM Handbook*, vol. 17, pp. 689–701, 1989.

[44] C. R. A. Schneider and J. R. Rudlin, "Review of statistical methods used in quantifying NDT reliability," *Insight—Non-Destructive Testing and Condition Monitoring*, vol. 46, no. 2, pp. 77–79, 2004.

[45] X. Guan, J. Zhang, K. Kadau, and S. Zhou, "Probabilistic fatigue life prediction using ultrasonic inspection data considering equivalent initial flaw size uncertainty," in *Review of Progress in Quantative Nondestructive Evaluation*, D. O. Thompson and D. E. Chimenti, Eds., vol. 32, pp. 620–627, American Institute of Physics, Melville, NY, USA, 2013.

[46] J. H. Kurz, A. Jüngert, S. Dugan, G. Dobmann, and C. Boller, "Reliability considerations of NDT by probability of detection (POD) determination using ultrasound phased array," *Engineering Failure Analysis*, vol. 35, pp. 6090–617, 2013.

[47] X. Guan, J. He, R. Jha, and Y. Liu, "An efficient analytical Bayesian method for reliability and system response updating based on Laplace and inverse first-order reliability computations," *Reliability Engineering & System Safety*, vol. 97, no. 1, pp. 1–13, 2012.

[48] S. L. Huang, Z. Wei, W. Zhao, and S. Wang, "A new omni-directional EMAT for ultrasonic lamb wave tomography imaging of metallic plate defects," *Sensors*, vol. 14, no. 2, pp. 3458–3476, 2014.